A first principles theoretical study of the hydration structure and dynamics of an excess proton in water clusters of varying size and temperature

ARTICLE *in* CHEMICAL PHYSICS · AUGUST 2011

Impact Factor: 1.65 · DOI: 10.1016/j.chemphys.2011.07.008

2 AUTHORS, INCLUDING:

Arindam Bankura
Temple University
12 PUBLICATIONS **104** CITATIONS

Chemical Physics 387 (2011) 92–102

Contents lists available at ScienceDirect

Chemical Physics

journal homepage: www.elsevier.com/locate/chemphys

A first principles theoretical study of the hydration structure and dynamics of an excess proton in water clusters of varying size and temperature

Arindam Bankura [1], Amalendu Chandra *

Department of Chemistry, Indian Institute of Technology, Kanpur 208016, India

ARTICLE INFO

Article history:
Received 12 May 2011
In final form 6 July 2011
Available online 18 July 2011

Keywords:
Excess proton
Water clusters
Ab initio molecular dynamics
Surface solvation
Vibrational spectrum
Proton transfer

ABSTRACT

We present a theoretical study of the structure and dynamics of protonated water clusters by means of quantum chemical calculations and *ab initio* molecular dynamics simulations. We have considered the clusters $H^+(H_2O)_n$ for four different sizes corresponding to $n = 5$, 9, 17 and 21. We have first looked at the solvation states of the excess proton in several lower energy structures of these clusters with a special interest in finding its surface versus interior states and its hydrogen bonding environment. Subsequently, we have investigated the finite temperature behavior of these clusters through *ab initio* simulations. We have looked at vibrational spectral features with special emphasis given to the spectral features of free OH (deuterated) modes and their dependence on donor–acceptor hydrogen bonding states of the water molecules. We have also investigated the mechanism and kinetics of proton transfer events in these clusters by using a population correlation function approach.

1. Introduction

Studies of neutral and charged water clusters have been a topic of great current interest because of their fundamental importance in many areas of science such as solvation chemistry, biochemistry and atmospheric science [1–4]. Protonated water clusters, in particular, are highly relevant in biological sciences, especially in cases where water molecules in a finite-sized environment are expected to behave differently from bulk water. The condensation of water droplets on ions is of central importance in atmospheric chemistry. Formation of the noctilucent clouds can take place in the atmosphere in presence of protonated water clusters through ion-induced nucleation mechanism [5]. For an acid–base reaction occurring in an aqueous medium of the type $HX_{(aq)} = H^+_{(aq)} + X^-_{(aq)}$, accurate characterization of the structural and dynamical aspects of the solvated proton is a rather difficult task. Studies of protonated water clusters in this context can provide very useful information of the structural and dynamical behavior of these excess protons. Indeed, there have been a rather large number of studies on protonated water clusters, both experimentally and theoretically, over past 2–3 decades. Mass-spectrometric studies [6–8] provided evidence for the existence of protonated water clusters $H^+(H_2O)_n$, some of which are more stable than others. For example, $n = 21, 28, 30, 37, 50\ldots$ are known as 'magic numbers' [6–11]. These magic number clusters have long been believed to be polyhedral cage structures enclosing either a water molecule or an H_3O^+ ion inside the cage. Information on hydration structure of an excess proton in $H^+(H_2O)_n$ has been experimentally obtained by high resolution infrared (IR) spectroscopy [12–19]. The structural information content is quite limited in the hydrogen bonded OH stretching region because of the breadth and congestion of the absorption bands in the spectra whereas the non-hydrogen-bonded or free OH stretching band is relatively sharp and well separated from the broad hydrogen-bonded OH absorption at $3000 \sim 3600\ cm^{-1}$. The frequency of a free OH stretching band appeared at $3600 \sim 3750\ cm^{-1}$ and the presence of these free OH modes contains useful information about the structure of these clusters. Furthermore, the free OH frequencies are different for water molecules in different hydrogen bonding environments. For example, a three-coordinated H_2O acting as a double-proton-acceptor and single-proton-donor (AAD), a two-coordinated H_2O acting as a single-proton-acceptor/single-proton-donor (AD) or double-proton-acceptor (AA), and a one-coordinated H_2O acting as a single-proton-acceptor (A) or a single-proton-donor (D) have different frequencies for their free OH modes. Using this concept, Yeh et al. [12] and Jiang et al. [13] conducted pioneering IR spectroscopic investigations on small to medium sized $H^+(H_2O)_n$ ($n \leqslant 8$) clusters. They reported vibrational spectra of these clusters and interpreted their results with the help of *ab initio* calculations. Headrick and coworkers [15] showed how the vibrational spectrum of protonated water clusters evolves in the size range from $n = 2$ to 11 due to local environment of the excess proton. From the distinct spectral changes in the free-OH stretching region, it is found that the

* Corresponding author. Fax: +91 512 2597436.
E-mail address: amalen@iitk.ac.in (A. Chandra).
[1] Present address: Department of Chemistry, Institute for Computational Molecular Science, Temple University, PA 19122, USA.

0301-0104/$ - see front matter © 2011 Elsevier B.V. All rights reserved.
doi:10.1016/j.chemphys.2011.07.008

structure of the cluster ions retains a chain like topology up to $n = 6$, the single-ring isomer first appears at $n = 7$ and the cage-like topology first appears at n = 11. Shin et al. [16] and Miyazaki et al. [17] recorded the IR spectra of protonated water clusters $H^+(H_2O)_n$ with n up to 27. These authors independently showed that the spectral features of the dangling OH stretch of water molecules change with increasing cluster size and it was concluded that three distinct morphological forms exist in protonated water clusters. Protonated clusters with less than ten water molecules form two dimensional chain and ring type structures. For clusters containing 10–21 water molecules, the hydrogen-bond network forms a two-dimensional net type structure to three-dimensional cage like structure with increasing number of water. The magic number cluster $H^+(H_2O)_{21}$ has been the subject of substantial interest to experimentalists [6–11,16,17]. Johnson and co-workers [16] reported that the infrared spectrum of $H^+(H_2O)_{21}$ in the free OH stretching region has only a single line at $\sim$3695 cm^{-1}, thus showing that all the water molecules of $H^+(H_2O)_{21}$ with a dangling OH are in similar binding state (AAD). However, in the study of Miyazaki and co-workers [17] on $H^+(H_2O)_{21}$ in a warmer molecular beam, the presence of two absorption bands in the same frequency range were found which meant the existence of two different binding types of water molecules in the cluster with a dangling OH. More recently, Mikami and coworkers [19] reported an IR spectroscopic study of size-selected protonated water clusters $H^+(H_2O)_n$ over a wider range of $n = 15$–100.

Size-selective protonated water clusters have also been investigated theoretically [3,13–16,19–47] in recent years. In order to elucidate the hydration structure of the excess proton and its transfer mechanism, a large number of different models have been employed ranging from empirical potentials [3,20–34] to *ab initio* [13–16,19,27,34–47] studies. Hodges and wales [21] obtained the global-minimum structures of protonated water clusters for $n = 2$–21. Their calculations showed a propensity in structural transition from tree-like geometries at $n = 2$–4 to four-membered and five-membered rings at $n \geqslant 5$, to cage-like configurations at $n \geqslant 9$, and finally to a distorted pentagonal dodecahedral cage enclosing a neutral water molecule at $n = 21$. While a great deal of efforts have been given on investigations of the global minima structures of different sized protonated clusters either by *ab initio* methods or by empirical models, less attention has been paid to investigate the finite temperature behavior of these clusters. It may be noted that the protonated water clusters in laboratory experiments or in atmosphere are not at zero temperature. Schindler et al. [48] estimated the temperature of their cluster to be near 140 K, while Jiang et al. [13] reported their cluster temperature to be about 170 K. The temperature of polar stratospheric cloud particles has been estimated to be $\sim$190 K [49]. In order to study the finite temperature behavior of these clusters, several molecular simulations [3,10,23–25,27,28,31–39,44,45] have been carried out on $H^+(H_2O)_n$ over different temperature ranges. Special emphasis has been placed on solid-like to liquid-like phase transitions by several authors using both Monte Carlo [3,10,23–25,27] and molecular dynamics [28,31–39,43–45] methods. To understand the thermal properties of protonated water clusters, simulations in the grand canonical ensemble have also been carried out at 250 K [28]. Singer et al. [25] and Christie et al. [26] examined the temperature dependence of the topology of $n = 6$, 8 and 16 clusters and they found that the major structural transitions involve reorganization of structures with treelike topology to ring-containing structures. Klein and coworkers [8] focused on examining finite temperature effects on the structure of $H^+(H_2O)_n$ ($n = 5$–22) using the parallel tempering method with OSS2 model [30]. Their calculated trends of global minima structures were found to be qualitatively similar to the results by Hodges and Wales [21]. However, all the clusters were found to undergo significant structural changes due to finite temperature effects. The structural and vibrational properties of the protonated clusters at finite temperature have also been studied by Kim and co-worker [46] for $n \leqslant 10$ by using quantum chemical calculations and *ab initio* molecular dynamics simulations. Their calculated vibrational spectra were found to be consistent with experimental observations. Recently, the structure, dynamics, and vibrational spectra of a hydrated proton in water clusters of $n = 21$, 31, 41, 51 have been studied at two different temperatures by using the *ab initio* atom-centered density matrix propagation simulations [34]. Based on the results of these finite temperature simulations, it was concluded that the protonated species in these clusters resides on the surface rather than being completely solvated in the interior. A detailed analysis of the vibrational properties of protonated clusters were also carried out and compared with the experimental findings. It was concluded that the dynamical and finite-temperature effects play a significant role in determining the vibrational spectral properties of these systems.

Another important aspect of these protonated water clusters is the rate of proton transfer in such finite-sized systems and to what extent the mechanism of proton transfer in these finite-sized clusters differs from that in bulk water. Majority of the existing theoretical studies on protonated water clusters focused on either the global minimum structures of these clusters or on how the overall structures change due to finite temperature effects. A few theoretical calculations have looked at the dynamics and mechanism of proton transfer in these clusters [31,34,45]. Much more work is needed in this area to have a better understanding of the hydration and translocation of excess protons in nano-sized hydrogen bonded clusters. One of our aims in this work is to provide a unified study of the structural and vibrational properties and also the rate and mechanism of proton transfer in these protonated clusters at finite temperature. In this context, it would also be worthwhile to investigate how the cluster properties depend on the cluster size and temperature. *Ab initio* molecular dynamics methods appear to be particularly useful in the elucidation of the proton transport mechanism which can depend strongly on both the local solvation environment of the ion and the hydrogen bonding fluctuations in the surrounding water molecules [50–52]. In this work, we have investigated some of the lower energy structures of selected protonated water clusters by means of quantum chemical calculations and then the dynamical properties of these clusters are investigated by *ab initio* molecular dynamics simulations. We have also calculated the probability distributions of hydrogen bonding states of water molecules and the hydronium ion and also vibrational frequencies from finite temperature simulations. In addition, the rates of proton transfer processes have been calculated by using the population correlation function approach [53,54]. The rate of proton transfer is found to vary significantly with cluster size for the clusters considered in this study.

The rest of the paper is organized as follows. The computational details of quantum chemical and *ab initio* molecular dynamics calculations are described in Section 2. Our results of the optimized geometries, hydration structures and vibrational power spectra are presented in Section 3. The kinetics and mechanism of proton migration in the present clusters are discussed in Section 4. Finally, our main results and conclusions are briefly summarized in Section 5.

2. Computational methods

We first carried out all-electron quantum chemical calculations of $H^+(H_2O)_n$ ($n = 5$, 9, 17 and 21) clusters to find the location of the excess proton in some of the low energy isomers of the clusters. All quantum chemical calculations were done at the post-Hartree–Fock *ab initio* level using the Möller–Plesset second order (MP2) perturbation theory that includes electron correlation effects and

also at density functional theory (DFT) level using the gradient corrected exchange–correlation functionals of BLYP[55,56] and B3LYP[56,57]. The Gaussian atomic basis set 6–31 + G* is used for the molecular orbital expansion which contains extra diffuse functions. The calculations were carried out using the GAUSSIAN 03 program [58]. In calculating the stabilization energies of the protonated clusters, we accounted for the basis set superposition error (BSSE) by using the so-called counterpoise method [59].

The *ab initio* molecular dynamics simulations were performed by means of the Car–Parrinello method [60,61] and the CPMD code [62]. A simple cubic box of length L containing an excess proton immersed in a cluster of n water molecules was taken in isolation for carrying out the simulations. Four different cluster sizes of n = 5, 9, 17 and 21 with box lengths of L = 15, 16, 18 and 18.52 Å, respectively, were used. In each case, the cluster was kept in the central region of the box and the length of the box was taken to be sufficiently large so that there was enough empty space around the cluster in all directions. The electronic structure was represented within the Kohn–Sham (KS) formulation [63] of density functional theory within a plane wave basis. The core electrons were treated via the Troullier–Martins normconserving pseudopotentials [64] and the plane wave expansion of the KS orbitals was truncated at a kinetic energy of 70 Ry. A time step of 5.0 a.u. along with an fictitious electron mass parameter μ = 800 a.u. were employed. In order to reduce the importance of nuclear quantum effects associated with the protons, all protons in the system were given the mass of deuterium. Also, the use of deuterium mass in place of hydrogen ensures that electronic adiabaticity and energy conservation are maintained throughout the simulations for the chosen values of the fictitious electronic mass parameter and time step. We note that this mass assignment does not affect the structural properties, hence we will continue to use the nomenclature of 'H' rather than 'D'. However, dynamical properties such as intramolecular vibrational features change due to deuterium mass assignment and, hence, an explicit mention of deuterium is made when such dynamical results are discussed. The *ab initio* MD simulations have been performed using the BLYP [55,56] functional. We note that this functional has been used in many earlier *ab initio* molecular dynamics studies of hydrogen bonded systems such as water, [65–69], methanol [70] and also ammonia [71–73]. We equilibrated the systems for about 8 ps in NVT ensemble using Nose–Hoover chain method at 300 K and, thereafter, we continued the runs in NVE ensemble for another 20–25 ps for calculations of the various structural and dynamical quantities. For n = 21, we also performed an additional simulation at a lower temperature of 150 K.

3. Structural properties and vibrational frequencies

In this section, we present the structural and vibrational spectral properties of different protonated water clusters considered here. It is known from previous studies that the lowest energy structures of these protonated water clusters transform from one dimensional chain to three dimensional cage through two dimensional ring type structures with increasing cluster size. Here we first describe some of the lower energy structures that we have obtained from quantum chemical calculations at BLYP, B3LYP and MP2 levels. Subsequently, the results of our *ab initio* molecular dynamics simulations will be discussed.

In order to identify the oxygen to which the excess proton is attached for a given configuration, we first assign to each oxygen its two nearest hydrogen atoms. Then the hydrogen that is left out is identified as the excess proton and it is then assigned to its nearest oxygen and this particular oxygen is identified as the hydronium oxygen O* [45,52,53]. The hydration structure of the hydronium ion in our molecular dynamics simulations is investigated by calculating the number of water molecules in its first hydration shell i.e., the coordination number N_{O*} and also by counting the number of hydrogen bonds that are donated through its three hydrogens i.e. hydrogen bond number N_{HB}. The hydrogen bonds are calculated by using a cut-off of 2.5 Å for the hydrogen–oxygen distance of two neighbouring molecules and an oxygen–oxygen cut-off distance of 3.5 Å is used for the first solvation shell to calculate the coordination number. We note that in our finite temperature simulations, the excess proton is not attached to a given oxygen for the entire trajectory due to the presence of proton transfer events. Hence, the index of the hydronium oxygen O* changes along the simulation trajectory.

We have also calculated the distributions of hydrogen bonding states of all water molecules present in the clusters. The state of a water molecule in the clusters can be very different from that in the bulk phase. A water molecule in the bulk phase is mostly fourfold coordinated where it accepts two hydrogen bonds and donates two hydrogen bonds i.e. double-acceptor and double-donor (AADD) type whereas water molecules in clusters can be one to four-coordinated. Depending on the number of acceptor–donor hydrogen bonds, the state of a water molecule in a cluster can be one-coordinated A or D, two-coordinated AA, DD or AD and three-coordinated AAD or ADD type. The vibrational properties of the clusters are found out by the calculating the Fourier transform of the velocity-velocity time correlation functions of all the atoms which are obtained from *ab initio* simulations. The velocity time correlation functions of the hydrogen atoms captures signatures of their hydrogen bonding states. The Fourier transform of the velocity time correlation function produces the power spectrum or the vibrational density of states

$$S(\omega) = \int_0^\infty C(t)cos\omega t dt. \quad (1)$$

We note that the hydrogen bonded OD stretching frequencies are much less than that of the free water or free OD vibrational frequencies. Normally, the non hydrogen bonded or free OD frequencies appear above 2450 cm^{-1} whereas the hydrogen bonded OD frequencies typically appear below 2400 cm^{-1}.

3.1. $H^+(H_2O)_5$

We first discuss the results of quantum chemical calculations of geometry optimizations. Out of the many geometries that we have explored for $H^+(H_2O)_5$, we have shown the four most stable structures in Fig. 1. These include one open, noncyclic, chain type structure HW5I, two four membered ring type structures of symmetric HW5II and asymmetric HW5III and one five membered ring type structure HW5IV. In the chain type structure, three water molecules are A type and one water molecule is AD type. In the four membered ring structures, one A type, one AA type and two AD type water molecules are found to be present. One AA type and two AD type water molecules are present in the five membered ring. The hydronium ion forms threefold coordinated Eigen cation $H_9O_4^+$ in the chain type and four membered ring type structures whereas it exists in a two-coordinated state in the five membered ring. Both B3LYP and MP2 calculations favour the symmetric single four membered ring (HW5II) structure over the chain type (HW5I) and five membered ring type (HW5IV) structure (see Table 1). It is found that HW5II is more stable than HW5I, HW5III and HW5IV by 0.65, 2.35 and 4.32 kcal/mol, respectively, at the B3LYP level. The ring type HW5III structure is found to transform to chain type HW5I structure in our MP2 calculations. Also, for MP2, the four member ring type HW5II is more stable than HW5I and HW5IV structures by 0.98 and 5.23 kcal/mol, respectively. Our BLYP results also show that the ring type (HW5II) structure is more stable than

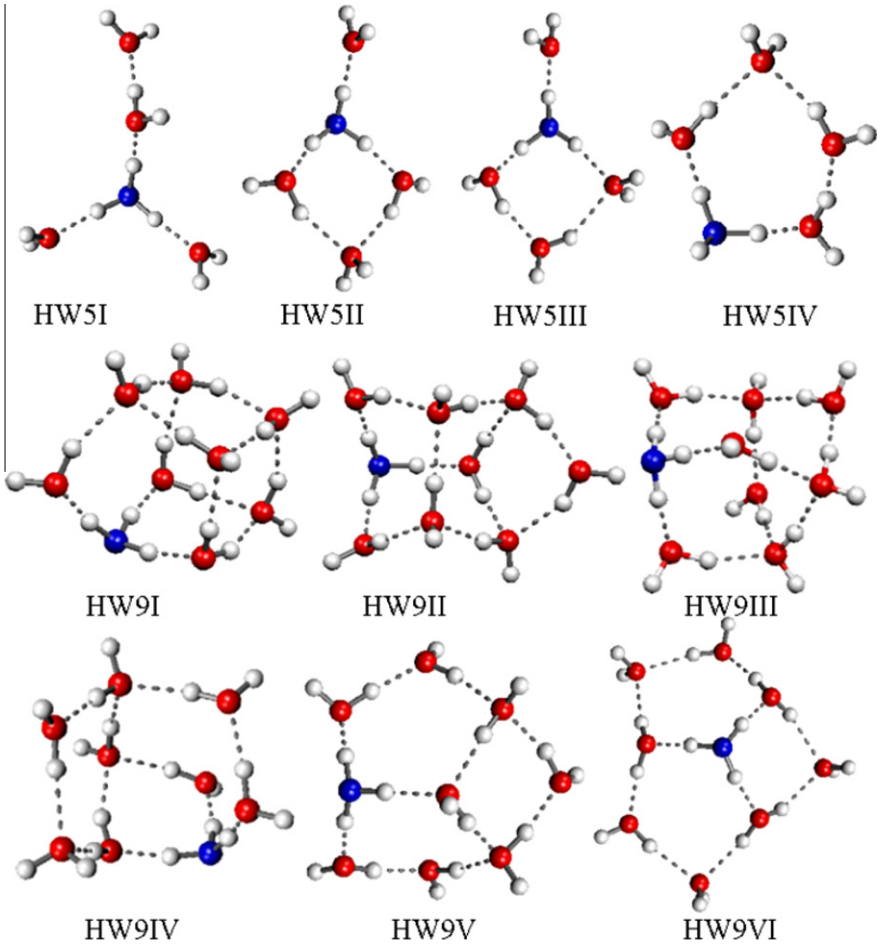

Fig. 1. Low energy structures of protonated water clusters $H^+(H_2O)_n$ for $n = 5$ and 9. The hydronium oxygen is the one that is covalently bound to three hydrogens.

Table 1
The stabilization energies of various optimized structures of $H^+(H_2O)_n$ clusters as obtained from all-electron quantum chemical calculations. All calculations are done with the 6–31 + G* basis set. The energy values are expressed in units of kcal/mol.

Isomer	BLYP	B3LYP	MP2
HW5I	−90.32	−92.09	−87.53
HW5II	−90.74	−92.74	−88.51
HW5III	−88.56	−90.39	–
HW5IV	−86.89	−88.42	−83.28
HW9I	−140.55	−144.88	−137.31
HW9II	−140.08	−144.62	−136.97
HW9III	−140.25	−144.49	−135.84
HW9IV	−137.85	−141.71	−135.40
HW9V	−138.95	−142.58	−134.19
HW9VI	−134.84	−138.90	−132.82
HW17I	−228.45	−238.40	−226.30
HW17II	−229.70	−238.27	−223.63
HW17III	−226.73	−235.20	−221.03
HW21I	−274.11	−293.11	−276.69
HW21II	−262.72	−282.81	−267.43
HW21II	−266.58	−286.27	−270.34

the other isomers. We note in this context that Jiang et al. [13] reported the chain type structure to be more stable than the ring type structure whereas Hodges et al. [21] have reported the ring type structure to be the global minimum structure for this cluster.

At finite temperature, configurations evolve from one structure to another giving rise to a distribution of hydrogen bonding states of water molecules. Such a distribution as obtained from our *ab initio* simulations is shown in Fig. 2(a). We see that three water molecules are in A state, one water molecule remains in AD state and the hydronium ion is in DDD state. Thus, the chain type structures are found to be preferred at finite temperature. Fig. 3(a) shows the power spectra of vibrational frequencies of the $H^+(H_2O)_5$ cluster. The sharpest features appearing near 2450 cm^{-1} and 2535 cm^{-1} are attributed to symmetric and asymmetric stretching vibrations of single coordinated A type water molecules. For the two-coordinated AD type water molecules, free OD stretching frequency appears at ~2515 cm^{-1} and the hydrogen bonded OD frequency appears at less than 2400 cm^{-1}. The OH stretching modes that are involved in hydrogen bonds are red-shifted and are also broadened considerably with respect to the free OH stretching bands. The experimental spectra for the symmetric and asymmetric OH stretching bands appear at 3650 and 3740 cm^{-1} for one-coordinated A type H_2O molecules and the free OH stretching band appears at 3715 cm^{-1} for two-coordinated AD type H_2O molecules [17]. A comparison of the experimental vibrational spectra of $H^+(H_2O)_5$ with our calculated power spectra clearly favours dominance of HW5I type structures as was also supported by the distributions of hydrogen bonding states (Fig. 2(a)). In Fig. 4, we have shown the hydronium oxygen index O*, the values of the coordination number (N_{O^*}) and hydrogen bond number (N_{HB}) of the hydronium ion along the simulation trajectory. The average values of these hydration numbers are: $N_{O^*} = 2.92$ and $N_{HB} = 2.92$. We observed both from quantum chemical as well as from *ab initio* molecular dynamics calculations that the hydronium ion prefers to donate three hydrogen bonds through its three hydrogens but it does not accept any hydrogen bond through its oxygen. Both three-coordinated $H_9O_4^+$ (Eigen cation) and a shared proton $H_5O_2^+$

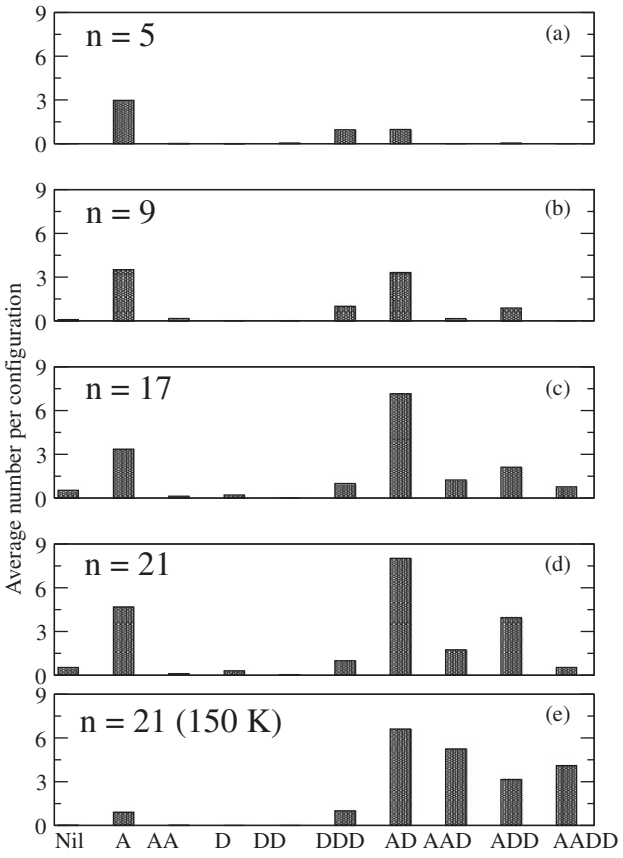

Fig. 2. Distributions of the hydrogen bonding states of water molecules and the hydronium ion in protonated water clusters at finite temperature. The results are for: (a) $H^+(H_2O)_5$, (b) $H^+(H_2O)_9$, (c) $H^+(H_2O)_{17}$, (d) $H^+(H_2O)_{21}$, all at 300 K and (e) $H^+(H_2O)_{21}$ at 150 K.

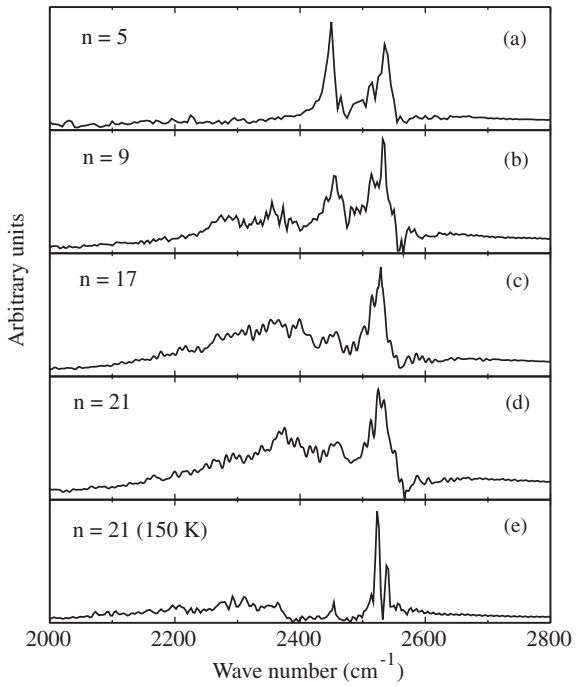

Fig. 3. Vibrational power spectra of $H^+(H_2O)_n$ in the stretching region of OH (with deuterium mass for hydrogen atoms). (a) $H^+(H_2O)_5$, (b) $H^+(H_2O)_9$, (c) $H^+(H_2O)_{17}$, (d) $H^+(H_2O)_{21}$, all at 300 K and (e) $H^+(H_2O)_{21}$ at 150 K.

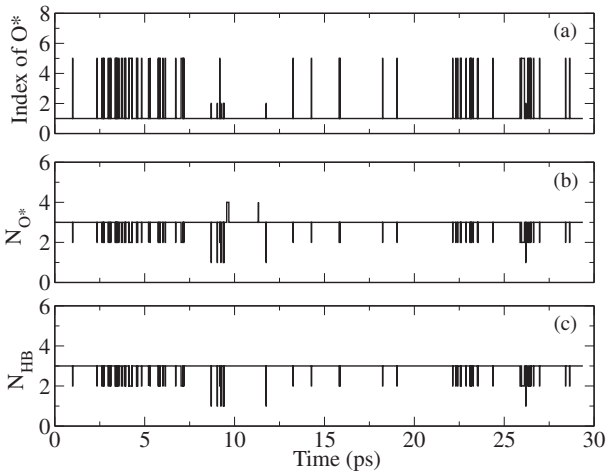

Fig. 4. Changes of the (a) index of the hydronium oxygen O*, (b) coordination number (N_{O^*}) and the (c) hydrogen bond number (N_{HB}) of the hydronium ion along the simulation trajectory for $H^+(H_2O)_5$ at 300 K.

(Zundel cation) are observed in the simulation with relative weights of 95% and 5%, respectively. For Eigen and Zundel cations, the average distances between the hydronium oxygen and the nearest water oxygen (R_{O^*O}) in the first solvation shell are found to be 2.54 and 2.44 Å, respectively.

3.2. $H^+(H_2O)_9$

In Fig. 1, we have shown some of the low energy structures of $H^+(H_2O)_9$ cluster that are found in the present study through geometry optimizations. The corresponding stabilization energies are included in Table 1. The lowest energy isomer (HW9I) is found to have a three-dimensional distorted cubic structure with two five and four four-membered rings which is in agreement with previous studies [8,21]. This isomer has six dangling hydrogens out of which one comes from the AD type water and other five belong to the five AAD type waters. Another stable structure (HW9II) is found to have a three-dimensional structure with seven dangling hydrogens from seven waters out of which three belong to two-coordinated AD type and other four belong to three-coordinated AAD type waters. The HW9II isomer is only 0.3–0.4 kcal/mol higher in energy than the HW9I at BLYP and B3LYP levels. The MP2 calculations predict a stronger stability of the HW9I isomer than HW9II. All other isomers have eight dangling hydrogens. HW9III and HW9IV have three dimensional structures whereas isomers of HW9V and HW9VI are found to have two-dimensional net or tree type structures. Our quantum chemical calculations predict that the HW9III isomer is higher in energy than HW9I by only 0.25–0.5 kcal/mol, while the isomer HW9IV is found to be 2–3 kcal/mol higher in energy. The isomer HW9III contains two six membered and two five membered rings where all the eight water molecules have one free hydrogen, five of them act as a two-coordinated AD type and the other three belong to three-coordinated AAD type waters. We note that Karthikeyan et al. [46] reported the HW9III isomer to be the lowest energy structure at B3LYP level while their MP2 calculations showed that the isomer HW9I is the most stable one. The two-dimensional HW9V and HW9VI isomers are found to be 2–6 kcal/mol higher in energy than that of the HW9I isomer. The isomer HW9V also has eight dangling hydrogens, five of them are due to AD type waters and rest three belong to AAD type water molecules. The isomer HW9VI has three AA type and two AD type water molecules, hence all the dangling hydrogens belong to two-coordinated water molecules.

In Fig. 2(b), we have shown the distribution of water molecules in different hydrogen bonding states for this cluster as obtained from the present simulation at room temperature. It is seen that mainly A, AD and ADD type water molecules are present in this cluster which means the two dimensional tree or net type structures are more dominant than the three dimensional structures for this cluster at finite temperature. A trace amount of AA and AAD type water molecules are also found which implies that sometimes ring type structure is also formed. In addition to the structures, we have also calculated the vibrational power spectrum from Fourier transforms of velocity auto-correlation functions and the results are shown in Fig. 3(b). The spectral peak frequency at $\sim$2533 cm^{-1} can be assigned to the asymmetric OD stretching mode of one-coordinated A type waters and the symmetric OD stretching vibration appears near 2455 cm^{-1}. These results can be linked to the experimental frequencies of $\sim$3740 cm^{-1} and $\sim$3650 cm^{-1} that were assigned to the asymmetric and symmetric stretching of A type water molecules for the corresponding protonated water clusters [14,17]. The peak near $\sim$2515 cm^{-1} appears from the two-coordinated AD type water molecules. Again, this peak can be linked to the experimental peak at $\sim$3715 cm^{-1} for AD type waters found for the corresponding protonated water cluster[14,17]. In our calculated spectrum, the broad band below 2400 cm^{-1} originates from the hydrogen bonded OD modes.

In Fig. 5, we have shown the variation of the hydronium oxygen index O*, coordination number (N_{O^*}) and the hydrogen bond number (N_{HB}) of the hydronium ion for $H^+(H_2O)_9$ cluster with time along the simulation trajectory. It is found that the hydronium ion almost always donates three hydrogen bonds, one through each of its hydrogen atoms. The average values of these hydration numbers are: $N_{O^*} = 3.0$ and $N_{HB} = 3.0$. In our simulation, we find that the excess proton is predominately solvated as Eigen cation (91%) at the finite temperature considered here. The average distance between the first solvation shell water and the hydronium ion is found to be 2.54 and 2.44 for the Eigen and Zundel cations, respectively.

3.3. $H^+(H_2O)_{17}$

For this cluster also, we have obtained a number of optimized structures from quantum chemical calculations. Among these, three different types of structures are shown in Fig. 6. The cage type structure of HW17I is found to have the lowest energy which contains one three-coordinated water molecule trapped within cage cavity and the three-coordinated hydronium ion residing at the surface. There are eight free hydrogens in this structure. Hodge et al. [21] have also reported a very similar structure for the lowest energy isomer for this cluster. Another dodecahedral cage type structure (HW17II) is also found with the H_3O^+ unit at the surface and it has ten free hydrogens. We also present another less stable open three dimensional structure (HW17III) with 10 dangling hydrogens in order to compare the stability of the cage structures with open distorted structures. We note that the cage type structures are not stable at finite temperature. At B3LYP level, this HW17I isomer is more stable than the other isomers of HW17II and HW17III by 0.13 and 3.2 kcal/mol, respectively, whereas the difference is 2.67 and 5.27 kcal/mol at the MP2 level (see Table 1). Thus, our calculations predict that the energy of the open distorted structure is 3–5 kcal/mol higher than the global minimum structure. We started our *ab initio* molecular dynamics simulations with the global minimum cage like HW17I structure, however the cage melted during the equilibration phase. The distribution of the hydrogen bonding states of water molecules over the simulated trajectory is shown in Fig. 2(c). On average, the number of water molecules in A, AD, AAD, ADD and AADD state are 3.35, 7.15, 1.24, 2.72 and 0.77, respectively. The calculated vibrational power spectrum of $H^+(H_2O)_{17}$ cluster is shown in Fig. 3(c). The symmetric and asymmetric stretching vibrations of the one-coordinated A-type water molecules appear near 2445 cm^{-1} and 2530 cm^{-1}. Free OD stretching vibrations in the two-coordinated AD type and three-coordinated AAD type water molecules appear near 2514 cm^{-1} and 2500 cm^{-1}, respectively, whereas considerably broadened peak for the hydrogen bonded OD modes appears at frequencies less than 2400 cm^{-1}. For this cluster, we see two broad peaks between 2350 to 2420 cm^{-1} region due to the symmetric and asymmetric stretching vibrations of two-coordinated DD and three-coordinated ADD type water molecules. We note that in the IR experiments of the corresponding protonated water cluster [16,17], the free-OH stretch region shows two bands at 3695 and 3715 cm^{-1} due to the dangling OH stretches of AAD and AD water molecules, respectively, and the broad bands around 3600 cm^{-1} arise from the symmetric and antisymmetric stretching vibration of ADD water molecules. In Fig. 7, we have shown the changes of hydronium oxygen index O*, coordination numbers N_{O^*} and hydrogen bond numbers N_{HB} with time. The average values of these hydration numbers are: $N_{O^*} = 3.04$ and $N_{HB} = 2.99$. During the simulation, the excess proton is found to stay in Zundel form in 10% of the configurations while it stayed in Eigen form in rest of the configurations. The average distance between O* and the oxygen of the nearest water (R_{O^*O}) is found to be 2.45 and 2.53 Å for Zundel and Eigen complexes, respectively.

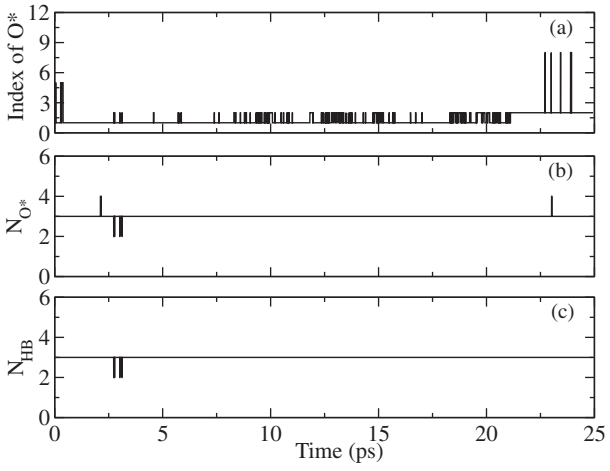

Fig. 5. Changes of the (a) index of the hydronium oxygen O*, (b) coordination number (N_{O^*}) and the (c) hydrogen bond number (N_{HB}) of the hydronium ion along the simulation trajectory for $H^+(H_2O)_9$ at 300 K.

3.4. $H^+(H_2O)_{21}$

Out of the many structures that we explored in our quantum chemical calculations, here we report three of them which have energies lower than others. These three structures are shown in Fig. 6. The lowest energy structure HW21I has nine dangling hydrogens, and an H_2O molecule inside the dodecahedral cage where the central H_2O forms four hydrogen bonds with the surface water molecules. We found another very similar structure HW21II with nine dangling hydrogens and the H_3O^+ ion residing inside the distorted dodecahedral cage. The central H_3O^+ ion forms three hydrogen bonds with the surface molecules and it is 11.39, 10.3 and 9.26 kcal/mol higher in energy than HW21I at BLYP, B3LYP and MP2 levels, respectively. Another lower energy structure HW21III is also found with ten dangling hydrogens with the H_3O^+ ion residing inside the dodecahedral cage and it is 6.84 and 6.35 kcal/mol higher in energy for B3LYP and MP2, respectively. On the basis of experimental findings and *ab initio* calculations

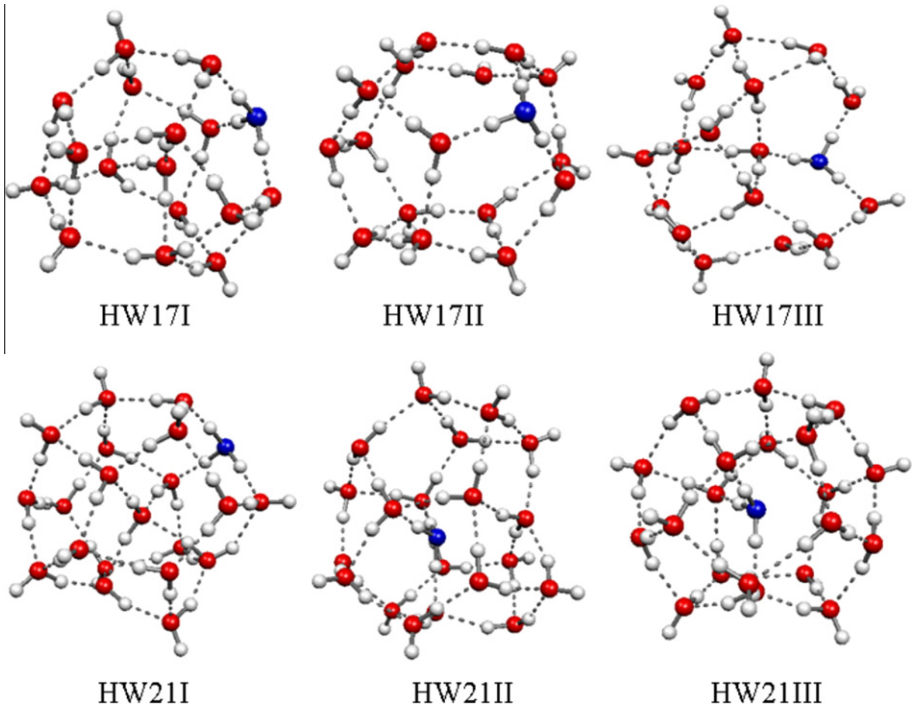

Fig. 6. Low energy structures of the protonated water clusters $H^+(H_2O)_n$ for $n = 17$ and 21. The hydronium oxygen is the one that is covalently bound to three hydrogens.

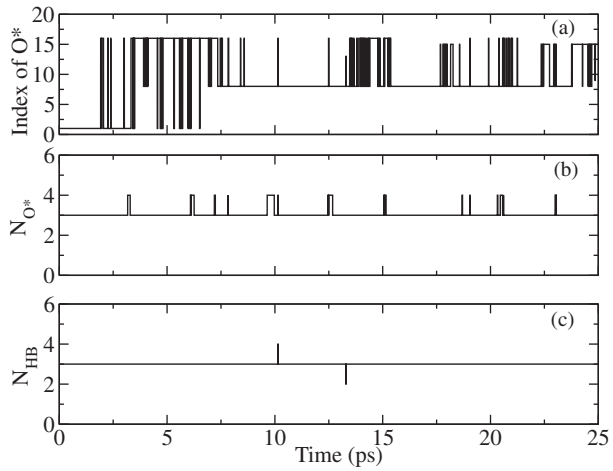

Fig. 7. Changes of the (a) index of the hydronium oxygen O*, (b) coordination number (N_{O^*}) and the (c) hydrogen bond number (N_{HB}) of the hydronium ion along the simulation trajectory for $H^+(H_2O)_{17}$ at 300 K.

[10,11,16,17,21,42], the most stable structure of the cluster with $n = 21$ has been suggested to be a regular dodecahedron cage that includes one water inside the cage. The isomer with interior H_3O^+ has also been reported [20,24] where all of the free OH modes belong to three-coordinated water molecules located in AAD environment. Both of the isomers of HW21I and HW21II have nine AAD type, six ADD type and five AADD type water molecules but HW21III has ten AAD type, seven ADD type and three AADD type water molecules. It may be noted that the experiments of Castleman et al. [11] suggested ten dangling hydrogen atoms in $H^+(H_2O)_{21}$ whereas the lowest energy isomer found in this study (HW21I) contains nine dangling hydrogens. Interestingly, relatively higher energy isomer HW21III with H_3O^+ ion inside the cage has ten dangling hydrogens which seems to indicate that experiments may not necessarily capture the lowest energy isomers due to their finite temperatures. Shin et al. [16] observed a single peak at 3695 cm^{-1} for free OH stretch suggesting that environments of all the dangling hydrogens are the same. This is also the case for HW21III. Hence, despite higher energy, the isomeric structure with H_3O^+ ion in the cage cavity rather than at surface seems to have the spectral features in agreement with experimental findings.

We started our *ab initio* molecular dynamics simulations with H_3O^+ ion inside the cage cavity at two different temperatures of 300 K and 150 K. The most probable structure of this magic number water cluster ion at 150 K is a distorted pentagonal dodecahedron with one H_2O molecule in the cage and a H_3O^+ ion on the surface. Raising the temperature partially melts the distorted pentagonal dodecahedron, converting some of the three-coordinated water molecules in the AAD configuration to two-coordinated water molecules in the AD configuration and one-coordinated water molecules in the A configuration. Fig. 2(d) and Fig. 2(e) show the average distribution of the hydrogen bonding states of water molecules at 300 and 150 K, respectively. In our simulations, the average numbers of water molecules in A, AD, AAD, ADD and AADD states are found to be 4.68, 8.15, 1.78, 3.97 and 0.53 at 300 K and the corresponding numbers are 0.9, 6.62, 5.24, 3.15 and 4.09 at 150 K. The temperature dependence of the calculated vibrational spectrum of $H^+(H_2O)_{21}$ in the OH stretching region is shown in Fig. 3(d) and Fig. 3(e) at 300 and 150 K, respectively. In Fig. 3(d), the appearance of the ~2450 and 2530 cm^{-1} bands corresponds to the symmetric and asymmetric stretching modes of one-coordinated water (A) molecules. The band near 2514 and 2504 cm^{-1} are characteristics of the free OD stretching of two-coordinated (AD) and three-coordinated (AAD) water molecules. The bonded symmetric and asymmetric OD stretching frequencies of two-coordinated DD and three-coordinated ADD type water molecules in the region 2350–2420 cm^{-1} are likely to be present but due to broadening their precise assignment has not been possible here. At 150 K, the symmetric and asymmetric stretching modes for A type water molecules are found to appear at ~2460 and 2540 cm^{-1}, respectively. Free OD stretching modes of AD and ADD type water molecules appear near 2524 and 2515 cm^{-1}, respectively, and the

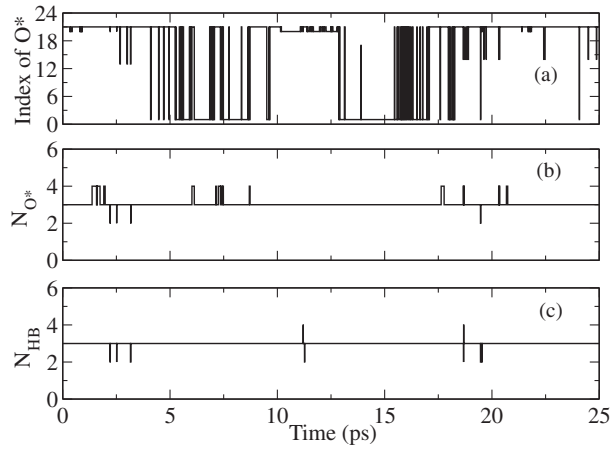

Fig. 8. Changes of the (a) index of the hydronium oxygen O*, (b) coordination number (N_{O^*}) and the (c) hydrogen bond number (N_{HB}) of the hydronium ion along the simulation trajectory for $H^+(H_2O)_{21}$ at 300 K.

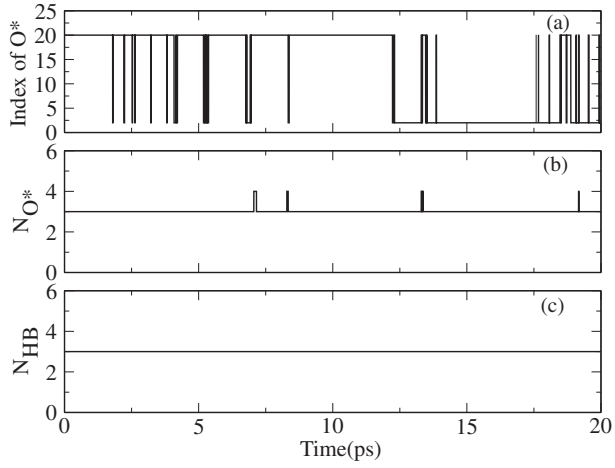

Fig. 9. Changes of the (a) index of the hydronium oxygen O*, (b) coordination number (N_{O^*}) and the (c) hydrogen bond number (N_{HB}) of the hydronium ion along the simulation trajectory for $H^+(H_2O)_{21}$ at 150 K.

symmetric and asymmetric stretching vibrations of ADD type water molecules appear in the region of 2300–2400 cm^{-1}. It may be noted that Miyazaki et al. [17] have shown that the vibrational predissociation spectrum of $H^+(H_2O)_{21}$ in the free OH stretching region contains a doublet at 3696 and 3717 cm^{-1} which was assigned to AAD and AD type water molecules.

The variation of the hydronium oxygen index O*, coordination number N_{O^*} and the hydrogen bond number N_{HB} with time at 300 K and 150 K are shown in Figs. 8 and 9, respectively. The calculated average values of these hydration numbers at the two temperatures are: N_{O^*} = 3.04, 3.04 and N_{HB} = 2.99, 2.99, respectively. The excess proton is found to be solvated in Zundel cation form in 11% of the configurations at 300 K and it stays in an Eigen complex form in rest of the configurations. The distance R_{O^*O} is found to be 2.45 and 2.54 Å for the Zundel and Eigen complexes, respectively. The fraction of configurations having the excess proton in Zundel cation form decreases to 5% at 150 K which is consistent with a slower rate of proton transfer at the lower temperature.

4. Kinetics of proton transfer

Proton transfer and charge migration kinetics in protonated water cluster systems are investigated by calculating appropriate proton transfer time-correlation functions [52–54] from the simulation trajectory. For this purpose, we define a population variable H (t) which is unity if the O* retains its identity continuously up to time t as it did at time t = 0 and it is zero otherwise. We construct the following continuous correlation function

$$C_c^{O^*O}(t) = \frac{\langle H(0)H(t)\rangle}{\langle H(0)^2\rangle}, \tag{2}$$

which gives the probability that the excess proton stays with the same oxygen continuously from time t = 0 to t. The associated integrated relaxation time τ_{exch} can be interpreted as the average lifetime of proton transfer (PT) and $1/\tau_{exch}$ would correspond to the average proton transfer rate. We note that the total proton transfer events have contributions from two kinds: Rattling where the excess proton returns to its original site after two successive proton transfer events and proton translocation where the excess proton moves to a different site after two successive proton transfer events. Clearly, the rattling events do not contribute to the overall net displacement of the excess proton. In computation of continuous proton transfer functions, rattling events can be either included or excluded. Since rattling occurs at a fast time scale, inclusion of such events would lead to faster decay of the correlation function compared to the one when such rattling events are excluded in the correlation function calculations. We have computed the correlation functions by both including and excluding the rattling events and the results are described below.

In Fig. 10, we have shown the decay of the PT correlation functions for all the clusters when rattling effects are included. The overall time constants of PT are shown in Table 2. It is seen that the rate of PT increases with increase of the cluster size. Also, for the same cluster size of n = 21, the PT rate is significantly slower at 150 K compared to that at 300 K. It is found that the overall decay of the proton transfer correlation functions including the rattling effects can be described well by a biexponential function with times constants τ_1 and τ_2 and corresponding weights a_1 and a_2 with $a_1 + a_2 = 1$. Our calculated results of the two time scales and their weights for all the clusters studied here are included in Table 2. In order to understand the origin of these two different time scales, we also calculated separately the PT correlation functions for Zundel and Eigen complexes separately and found time scales similar to τ_1 for the Zundel complex and τ_2 for the Eigen complex. Hence, the biexponential decay of the overall PT correlation function can be assigned to different decay rates of the Zundel and Eigen complexes. Using this framework, a comprehensive

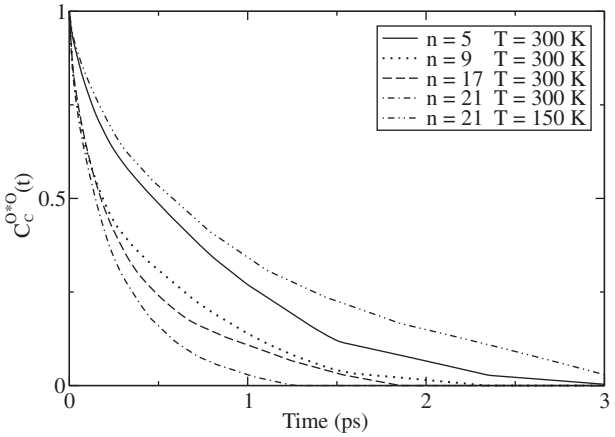

Fig. 10. Time dependence of the continuous proton transfer time correlation functions for $H^+(H_2O)_n$. The solid, dotted, dashed, dashed-dotted and the dashed-double dotted curves are for n = 5, 9, 17 and 21 at 300 K, and for n = 21 at 150 K, respectively.

Table 2
The time scales of proton transfer events as obtained from the decay of continuous correlation functions including rattling events. The two times scales as obtained from biexponential fits to the correlations are also included. All time scales are expressed in ps. Also note that deuterium mass has been used for all hydrogens in our calculations.

Cluster system	Temperature (K)	τ_1	τ_2	τ_{exch}
$H^+(H_2O)_5$	300	0.03	0.78	0.71
$H^+(H_2O)_9$	300	0.04	0.59	0.43
$H^+(H_2O)_{17}$	300	0.07	0.52	0.37
$H^+(H_2O)_{21}$	300	0.03	0.30	0.25
$H^+(H_2O)_{21}$	150	0.06	1.07	0.92

analysis of solvation shell structure, proton rattling and true proton transfer time scales have been performed in our cluster systems. Substantial experimental and theoretical investigations into the structural diffusion or Grothuss mechanism of the hydrated excess proton in bulk water are now available [50–52]. The proton transfer picture involves an interplay between a threefold coordinated complex 'Eigen cation' $H_9O_4^+$, and a shared proton complex 'Zundel cation' $H_5O_2^+$. According to the presolvation concept, the structural diffusion requires that for any proton transfer process, the proton receiving species must have a solvation pattern that corresponds to the species into which it will be transformed as a result of the reaction. Bulk water molecules prefer essentially a fourfold tetrahedral coordination shell whereas the hydronium ion prefers threefold coordination. Hydrogen-bond coordination number of one of the H_2O molecules in the first solvation shell is lowered by the breaking of a hydrogen bond to the second solvation shell, the reduction in coordination number of the first solvation shell water places this water in a coordination pattern similar to that of the $H_9O_4^+$ cation, thereby allowing the proton to transfer from the hydronium to this water via the interconversion process. The protonic charge is transferred from the H_3O^+ ion to the H_2O molecule with the reduced hydrogen bond coordination number, in which the Zundel structure occurs as an intermediate state. The rate-limiting step in the process is the time needed to reduce the coordination number, i.e. to break a water-water hydrogen bond. The time scales of breaking of such water-water hydrogen bonds can also be obtained by using the so-called hydrogen bond population correlation function approach [74–76]. A recent first principles study[54] reported a concerted mechanism for actual proton transfer events where the breakage of an acceptor hydrogen bond in the first solvation shell and the acceptance of a hydrogen bond by the hydronium ion take place in rapid succession. Still, the presolvation concept was found to retain substantial validity in explaining the mechanism of proton transfer in aqueous systems.

In clusters, hydronium ion prefers threefold DDD coordination type whereas the coordination number of water molecules can be one to four. So, even within the broad framework of presolvation concept, the details of the mechanism of proton transfer in clusters can be different from that in bulk water. We first discuss the smaller cluster $H^+(H_2O)_5$ which has mainly a chain type structure and the hydronium ion is three coordinated. In the first solvation shell, two water molecules are in one-coordinated A state and one water molecule is in two-coordinated AD state. If any proton transfer takes place to any of the water molecules in the first solvation shell, the coordination of the newly formed hydronium ion becomes onefold or twofold and the excess proton return to its original site immediately because one or two-coordinated hydronium is not stable and it always prefers a threefold coordination. So for this smaller cluster, the excess proton stays essentially all the time with the same oxygen. There are few transfer events in Fig. 4 due to proton rattling effects. The decay behavior of the correlation functions including rattling effects is shown in Fig. 10. A biexponential fit gives the following two time scales: $\tau_1 \approx 30$ fs and $\tau_2 \approx 780$ fs and the integrated average lifetime τ_{exch} of the excess proton with a given hydronium ion including rattling effects is found to be ≈710 fs (see Table 2).

Now we discuss the details of proton transfer kinetics in the medium sized cluster ($n = 9$). In this cluster, the H_3O^+ ion is again three-coordinated. The water molecules are two or three-coordinated with AD, AAD and ADD types. In this cluster, on average one water molecule is found in the three-coordinated ADD type. True proton transfer can only be possible, if this ADD type water molecule stays in the first solvation shell of the hydronium ion. There are few rattling and true proton transfer events occurring in this cluster (shown in Fig. 5). The decay behavior of the continuous correlation function $C_c^{O^*O}(t)$ including rattling events for the $H^+(H_2O)_9$ cluster is shown in Fig. 10. We found two time scales of $\tau_1 \approx 40$ fs and $\tau_2 \approx 590$ fs by fitting the decay curve to a biexponential function. Our calculations suggest that the short and long time scales are due to the rattling effects of the Zundel and Eigen complexes. The integrated average lifetime (τ_{exch}) is found to be ≈430 fs (see Table 2). When rattling effects are excluded, the average lifetime at 300 K is found to be 29.2 ps.

In bigger clusters of $H^+(H_2O)_n$ with $n = 17$ and 21, the lowest energy structures are cage like where water molecules remain mainly in the three-coordinated AAD/ADD type environments. However, such cage structures are found to be not stable at room temperature. The cages open up producing a mixture of one-coordinated A type, two-coordinated AD type and three-coordinated ADD/AAD type water molecules and form three dimensional network structures. For these bigger clusters, only three to four water molecules are found to be threefold (AAD or ADD) coordinated at 300 K. During the simulation period, water molecules mainly remain in threefold ADD or AAD coordination in the 1st solvation shell whereas other water molecules are one or two-coordinated. Only one or two molecules are found to be three-coordinated in the second solvation shell. After proton transfer, the environment of the newly formed hydronium ion should be three-coordinated but some of the water molecules in the first solvation shell are one or two-coordinated. So the chance of return of the excess proton to its original site is very high. Some major rearrangement of the overall cluster by reorganization of hydrogen bonds can create the three-coordinated water molecules in the first solvation shell and favours true proton transfer. Thus, we observe a slower rate of true proton transfer in clusters than that in bulk water.

The decay behavior of the correlation functions for $H^+(H_2O)_{17}$ cluster at 300 K is shown in Fig. 10. Proton rattling effects are included here. Upon fitting the decay behavior of $C_c^{O^*O}(t)$ to a biexponential function, we get one fast ($\tau_1 \approx 70$ fs) and one slow ($\tau_2 \approx 520$ fs) time scales. The integrated average lifetime (τ_{exch}) of the hydronium ion in $H^+(H_2O)_{17}$ is found to be ≈370 fs (see Table 2) when rattling effects are included. Again, calculations of the time scales separately for Zundel and Eigen complexes reveal that the faster and the slower time scales correspond to proton transfer events in Zundel and Eigen complexes, respectively. Exclusion of proton rattling events produces an average time scale $\tau_{exch} \approx 5.4$ ps which is significantly slower than the value we obtained upon inclusion of rattling events. Clearly, majority of the proton transfer events that occur are rattling events due to large amplitude intermolecular vibrations and only a few of them correspond to true proton translocations. Also, the rate of true proton transfer, although still slower than the bulk value, has increased compared to its values for the smaller clusters.

We have extracted the proton transfer rates for the $H^+(H_2O)_{21}$ cluster at both 300 and 150 K. The decay of the correlation functions for this cluster is shown in Fig. 10. It is seen that the rate of proton transfer in $H^+(H_2O)_{21}$ is slightly faster than that in $H^+(H_2O)_{17}$ at 300 K. Including proton rattling events, the two time scales are found to be: $\tau_1 \approx 30$ fs and $\tau_2 \approx 300$ fs and the average

proton transfer time constant is found to be: $\tau_{exch} \approx 250$ fs. Exclusion of proton rattling events gives a time scale of ~4.39 ps which is faster than that of the smaller clusters but still slower than the bulk result [53]. At the lower temperature of 150 K, the value of τ_{exch} changes to 0.92 ps including rattling effects and 28.1 ps excluding rattling effects. Clearly, the dynamics of proton transfer in clusters depends not only on the cluster size but also on the temperature of the clusters. For the $H^+(H_2O)_{21}$ system at 150 K, the cage structure melted only partially and water molecules in the first solvation shell are found to be in two, three or four-coordinated states in the partially melted cage structures. The presolvation concept requires that the proton receiving species must be in the three-coordinated ADD type hydrogen bonding state. So, some internal rearrangement of water molecules is required to bring a water molecule in the first solvation shell to the required three-coordinated ADD type state before a proton transfer can occur. Whereas at 300 K, all the water molecule in the first solvation shell remain in three-coordinated ADD state. Hence, the probability of proton transfer at 150 K is found to be much less compared to that at 300 K.

5. Conclusions

In this work, we have investigated the solvation structure and migration kinetics of an excess proton embedded in water clusters of different sizes at finite temperature. More specifically, we have looked at protonated clusters having 5, 9, 17 and 21 water molecules. First, many of the low energy structures of these clusters are studied by means of quantum chemical calculations and subsequently their finite temperature behavior is investigated by *ab initio* molecular dynamics simulations. Different structural isomers with not too different energies are found for these clusters. It is found that the symmetrical four-membered ring structure predominates over the open chain structure at room temperature for $n = 5$ case. The lowest energy structure of $n = 9$ is a three-dimensional distorted cubic type while two-dimensional tree or net type structures are found to be predominant at room temperature. For $n = 17$, although the clatherate cage structure with one water molecule in cage cavity and hydronium ion at surface is found to be the lowest energy structure, such cage structures are found to melt at room temperature giving rise to three dimensional open structures. Our quantum chemical calculations for the magic numbered water cluster ($n = 21$) predicts a cage structure with one water molecule in the cage cavity as the lowest energy structure. Our finite temperature *ab initio* molecular dynamics simulations reveal that the most probable structure of this magic number water cluster ion at 150 K is a distorted pentagonal dodecahedron with one H_2O molecule in the cage and the H_3O^+ ion on the surface. Raising the temperature to 300 K melts the distorted pentagonal dodecahedron by converting some of the three and four-coordinated water molecules to those with one and two hydrogen bonds.

The calculated vibrational power spectra from the velocity autocorrelation functions are found to have features that are comparable with the corresponding experimental IR spectra. Due to finite temperature effects, the cages are melted leading to changes in the hydrogen bonding state of water molecules. This, in turn, results in noticeable changes in the calculated spectra. In all cases, it is possible to distinguish the spectral features of water molecules of different hydrogen bonding environments, a key feature that has been used by the experimentalists to uncover the structure of these clusters. For example, in our study, the peak frequencies of non-hydrogen bonded or free OD stretching band are found to be at ~2530 cm^{-1} for one-coordinated A type, ~2515 cm^{-1} for two-coordinated AD type and at ~2500 cm^{-1} for three-coordinated AAD type water molecules.

Our *ab initio* molecular dynamics simulations reveal that the excess proton is mostly localized on a single water molecule forming a three-coordinated Eigen cation ($H_9O_4^+$). In some of the configurations, it is nearly equally shared by two water molecules yielding the so-called Zundel cation ($H_5O_2^+$). By using a population correlation function approach [52,53], explicit times scales are extracted for proton transfer kinetics. Calculations are done by both including and excluding the contributions of proton rattling effects. Expectedly, the dynamics is found to be faster when the rattling effects are included. The details of the proton transfer mechanism are found to differ from that in bulk water because of varying hydrogen bonding states of water in clusters. However, the mechanism can still be framed within the so-called presolvation concept from a broader perspective. It is observed that significant structural rearrangements of the clusters by breaking and reformation of hydrogen bonds can bring the solvation shell water molecules in three-coordinated ADD state which favours true proton transfer in these clusters. Since such three-coordinated water molecules are not available in the hydration shell very frequently, the rate of proton transfer in these clusters is found to be slower than that in bulk water. The rate of proton transfer is also found to slow down significantly when the temperature is decreased to 150 K from room temperature.

Acknowledgment

We gratefully acknowledge financial supports from Board of Research in Nuclear Sciences (BRNS) and Department of Science and Technology (DST), Government of India.

References

[1] C.K. Lutrus, D.E. Hagen, S.H. Salk, S. Atm. Environ. A 24 (1990) 1397.
[2] R.G. Keesee, J. Geophys. Res. 94 (1989) 14683.
[3] R. Kelterbaum, E. Kochanski, J. Phys. Chem. 99 (1995) 12493.
[4] C.E. Kolb, R.A. Cox, J.P.D. Abbatt, et al., Atmos. Chem. Phys. 10 (2010) 10561.
[5] X. Yang, A.W. Castleman Jr., J. Geophys. Res. 96 (1991) 22573.
[6] S.S. Lin, Rev. Sci. Instrum. 44 (1973) 516.
[7] X. Yang, X. Zhang, A.W. Castleman Jr., Int. J. Mass Spectrom. Ion Processes 109 (1991) 339.
[8] C.-C. Wu, C.-K. Lin, H.-C. Chang, J.-C. Jiang, J.-L. Kuo, M.L. Klein, J. Chem. Phys. 122 (2005) 074315.
[9] J.L. Kassner, D.E. Hagen, J. Chem. Phys. 64 (1976) 1860.
[10] U. Nagashima, H. Shinohara, N. Nishi, H. Tanaka, J. Chem. Phys. 84 (1986) 209.
[11] S. Wei, Z. Shi, A.W. Castleman Jr., J. Chem. Phys. 94 (1991) 3268.
[12] L.I. Yeh, M. Okumura, J.D. Myers, J.M. Price, Y.T. Lee, J. Chem. Phys. 91 (1989) 7319.
[13] J.-C. Jiang, Y.-S. Wang, H.-C. Chang, S.H. Lin, Y.T. Lee, G. Niedner-Schatteburg, H.-C. Chang, J. Am. Chem. Soc. 122 (2000) 1398.
[14] C.-K. Lin, C.-C. Wu, Y.-S. Wang, Y.T. Lee, H.-C. Chang, J.-L. Kuo, M.L. Klein, Phys. Chem. Chem. Phys. 7 (2005) 938.
[15] J.M. Headrick, E.G. Diken, R.S. Walters, N.I. Hammer, R.A. Christie, J. Cui, E.M. Myshakin, M.A. Duncan, M.A. Johnson, K.D. Jordan, Science 308 (2005) 1765.
[16] J.-W. Shin, N.I. Hammer, E.G. Diken, M.A. Johnson, R.S. Walters, T.D. Jaeger, M.A. Duncan, R.A. Christie, K.D. Jordan, Science 304 (2004) 1137.
[17] M. Miyazaki, A. Fujii, T. Ebata, N. Mikami, Science 304 (2004) 1134.
[18] G.E. Douberly, A.M. Ricks, M.A. Duncan, J. Phys. Chem. A 113 (2009) 8449.
[19] K. Mizuse, A. Fujii, N. Mikami, J. Chem. Phys. 126 (2007) 231101.
[20] R.E. Kozack, P.C. Jordon, J. Chem. Phys. 99 (1993) 2978.
[21] M.P. Hodges, D.J. Wales, Chem. Phys. Lett. 324 (2000) 279.
[22] T. James, D.J. Wales, J. Chem. Phys. 122 (2005) 134306.
[23] J.-L. Kuo, M.L. Klein, J. Chem. Phys. 122 (2005) 024516.
[24] M. Svanberg, J.B.C. Pettersson, J. Phys. Chem. A 102 (1998) 1865.
[25] S.J. Singer, S. McDonald, J. Chem. Phys. 112 (2000) 710.
[26] R.A. Christie, K.D. Jordan, J. Phys. Chem. B 106 (2002) 8376.
[27] C.V. Ciobanu, L. Ojamae, I. Shavitt, S. J. Singer J. Chem. Phys. 113 (2000) 5321.
[28] S.V. Shevkunov, A. Vegiri, J. Chem. Phys. 111 (1999) 9303.
[29] I. Kusaka, D.W. Oxtoby, J. Chem. Phys. 113 (2000) 10100.
[30] L. Ojame, I. Shavitt, S.J. Singer, J. Chem. Phys. 109 (1998) 5547.
[31] M. Gavagno, D. Laria, J. Rodriguez, J. Mol. Liq. 136 (2007) 317.
[32] H. Yu, Q. Cui, J. Chem. Phys. 127 (2007) 234504.
[33] C. Kobayashi, K. Iwahashi, S. Saito, I. Ohmine, J. Chem. Phys. 105 (1996) 6358.
[34] S.S. Iyengar, M.K. Petersen, T.J.F. Day, C.J. Burnham, V.E. Teige, G.A. Voth, J. Chem. Phys. 123 (2005) 084309;
S.S. Iyengara, T.J.F. Day, G.A. Voth, Int. J. Mass. Spectrom. 241 (2005) 197.

[35] D.Q. Wei, D.R. Salahub, J. Chem. Phys 101 (1994) 7633;
D.Q. Wei, D.R. Salahub, J. Chem. Phys. 106 (1997) 6086.
[36] H.-P. Cheng, J.L. Krause, J. Chem. Phys. 107 (1997) 8461.
[37] P.L. Geissler, C. Dellago, D. Chandler, J. Hutter, M. Parrinello, Chem. Phys. Lett. 321 (2000) 225.
[38] H.-P. Cheng, J. Phys. Chem. A 102 (1998) 6201.
[39] H.-P. Cheng, R.N. Barnett, U. Landman, Chem. Phys. Lett. 237 (1995) 161.
[40] A.L. SoboleWski, W. Domcke, J. Phys. Chem. A 106 (2002) 4158.
[41] A. Khan, Chem. Phys. Lett. 217 (1994) 443.
[42] A. Khan, Chem. Phys. Lett. 319 (2000) 440.
[43] K. Laasonen, M.L. Klein, J. Phys. Chem. 98 (1994) 10079.
[44] S.S. Iyengar, T.J.F. Day, G.A. Voth, Int. J. Mass. Spectrom. 241 (2005) 197.
[45] A. Bankura, A. Chandra, Pramana – J. Phys. 65 (2005) 763;
A. Bankura, A. Chandra, Proc. Ind. Nat. Sci. Acad. 71A (2007) 399.
[46] I. Shin, M. Park, S.K. Min, E.C. Lee, S.B. Suh, K.S. Kim, J. Chem. Phys. 125 (2006) 234305;
S. Karthikeyan, M. Park, I. Shin, K.S. Kim, J. Phys. Chem. A 112 (2008) 10120;
S. Karthikeyan, K.S. Kim, Mol. Phys. 107 (2009) 1169.
[47] N.J. Singh, M. Park, S.K. Min, S.B. Suh, K.S. Kim, Angew. Chem. Int. Ed. 45 (2006) 3795.
[48] T. Schindler, C. Berg, G. Niedner-Schatteburg, V.E. Bondybey, Chem. Phys. Lett. 229 (1994) 57.
[49] J. Schreiner, C. Voigt, A. Kohlmann, F. Arnold, K. Mauersberger, N. Larsen, Science 283 (1999) 968.
[50] D. Marx, M.E. Tuckerman, J. Hutter, M. Parrinello, Nature (London) 397 (1999) 601.
[51] D. Marx, Chem. Phys. Chem. 7 (2006) 1848;
D. Marx, Chem. Phys. Chem. 8 (2007) 209.
[52] M.E. Tuckerman, A. Chandra, D. Marx, Acc. Chem. Res. 39 (2006) 151;
D. Marx, A. Chandra, M. Tuckerman, Chem. Rev. 120 (2010) 2174.
[53] A. Chandra, M. Tuckerman, D. Marx, Phys. Rev. Lett. 99 (2007) 145901.
[54] T.C. Berkelbach, H.-S. Lee, M.E. Tuckerman, Phys. Rev. Lett. 103 (2009) 238302.
[55] A.D. Becke, Phys. Rev. A 38 (1988) 3098.
[56] C. Lee, W. Yang, R.G. Parr, Phys. Rev. B 37 (1988) 785.
[57] A.D. Becke, J. Chem. Phys. 98 (1993) 5648.
[58] M.J. Frisch, G.W. Trucks, H.B. Schlegel, et al., GAUSSIAN 03, Gaussian Inc., Pittsburgh, PA, 2003.
[59] F.B. Van. Duijneveldt, J.G.C.M. van Duijneveldt-van de Rijdt, J.H. van Leuthe, Chem. Rev. 94 (1994) 1873.
[60] R. Car, M. Parrinello, Phys. Rev. Lett. 55 (1985) 2471.
[61] D. Marx, J. Hutter, Ab Initio Molecular Dynamics: Basic Theory and Advanced Methods, Cambridge University Press, Cambridge, 2009.
[62] CPMD Program, J. Hutter, A. Alavi, T. Deutsch, M. Bernasconi, St. Goedecker, D. Marx, M. Tuckerman, M. Parrinello, MPI für Festkörperforschung and IBM Zurich Research Laboratory.
[63] W. Kohn, L.J. Sham, Phys. Rev. A 140 (1965) 1133.
[64] N. Troullier, J.L. Martins, Phys. Rev. B 43 (1991) 1993.
[65] K. Laasonen, M. Sprik, M. Parrinello, R. Car, J. Chem. Phys. 99 (1993) 9080.
[66] M. Sprik, J. Hutter, M. Parrinello, J. Chem. Phys. 105 (1995) 1142.
[67] P.L. Silvestrelli, M. Parrinello, Phys. Rev. Lett. 82 (1999) 3308.
[68] P.L. Silvestrelli, M. Parrinello, J. Chem. Phys. 111 (1999) 3572.
[69] B.S. Mallik, A. Semparithi, A. Chandra, J. Phys. Chem. A 112 (2008) 5104;
B.S. Mallik, A. Semparithi, A. Chandra, J. Chem. Phys. 129 (2008) 194512.
[70] E. Tsuchida, Y. Kanada, M. Tsukada, Chem. Phys. Lett. 311 (1999) 236.
[71] M. Diraison, G.J. Martyna, M.E. Tuckerman, J. Chem. Phys. 111 (1999) 1096.
[72] Y. Liu, M.E. Tuckerman, J. Phys. Chem. B 105 (2001) 6598.
[73] D. Boese, A. Chandra, J.M. Martin, D. Marx, J. Chem. Phys. 119 (2003) 5965.
[74] A. Luzar, D. Chandler, Phys. Rev. Lett. 76 (1996) 928;
A. Luzar, D. Chandler, Nature (London) 379 (1996) 55.
[75] A. Chandra, J. Phys. Chem. B 107 (2003) 3899;
S. Chowdhuri, A. Chandra, J. Phys. Chem. B 110 (2006) 9674.
[76] H. Xu, B.J. Berne, J. Phys. Chem. B 105 (2001) 11929;
H. Xu, H.A. Stern, B.J. Berne, J. Phys. Chem. B 106 (2002) 2054.